Q. J. R. Meteorol. Soc. (2005), **131**, pp. 1251–1270 doi: 10.1256/qj.04.66

Moisture fluxes over snow with and without protruding vegetation

By L. MAHRT* and D. VICKERS
Oregon State University, Corvallis, USA

(Received 6 May 2004; revised 21 December 2004)

SUMMARY

The sublimation of snow and evaporation of melted snow is contrasted between brush, grass and bare ground sites using eddy-correlation data. Averaged over the entire winter season, the evaporation/sublimation is about 20% greater over the brush site than the bare ground site, apparently due to greater supply of snow. Blowing snow collects in patches of brush, which protrude above the snow.

This study evaluates commonly used simple formulations of the surface moisture flux including two versions of the bulk aerodynamic formula and the stability-dependent Penman and Penman–Monteith methods for predicting evaporation/sublimation. The evaluation is based on eddy-correlation data from the three sites with conditions ranging from snow-free to snow-covered ground surfaces. The water availability factors, required for these formations, increase with snow-fraction coverage, but less so with melting conditions, depending on site and formulation. Various influences on the sublimation/evaporation are examined and the performance and shortcomings of each formulation are assessed.

KEYWORDS: Bulk aerodynamic Penman Snow melt Sublimation

1. INTRODUCTION

The presence of complete or partial snow cover substantially reduces or eliminates the daytime upward sensible heat flux through increased albedo and energy used to sublimate and melt snow and evaporate melted snow. Reduced upward heat flux leads to weaker turbulence and shallower boundary-layer depths.

The moisture flux due to sublimation and evaporation of melted snow behaves quite differently depending on whether the vegetation is completely covered by snow or not. Short vegetation protruding above the snow that is at least partly snow free can generate significant upward sensible heat flux. Partly or completely snow-free tall canopies can decouple the snow-covered ground surface from the atmosphere above the canopy (e.g. Davis *et al.* 1997; Hedstrom and Pomeroy 1998; Link and Marks 1999; Nakai *et al.* 1999; Pomeroy *et al.* 2003).

Complete snow cover without protruding vegetation has been studied more extensively (see references in Andreas 2002). The moisture flux above snow surfaces with short protruding vegetation has received less attention and is more complex. Sturm *et al.* (2001) and Liston *et al.* (2002) examined the ability of short vegetation to collect blowing snow and the subsequent influence on the surface energy budget, the feedback on the vegetation through moderation of soil temperatures and the implications for climate change. Evaluation of models with eddy-correlation measurements of moisture flux with partial snow cover is even less common (Yang *et al.* 1999).

For partial snow cover, a number of models have explicitly partitioned the influences of snow-free and snow-cover parts of the surface. Liston and Sturm (1998) and others have partitioned the roughness length for a grid area into snow-covered parts and snow-free parts. Liston (1995) recommends separate energy budgets for the snow-covered and snow-free fractions of each grid area. Essery *et al.* (2003) estimate the albedo as a weighted average of the snow-covered and snow-free parts of each subgrid area. Liston (2004) formulated the subgrid distribution of snow-depth and snow-cover

* Corresponding author: College of Oceanic and Atmospheric Sciences, Oregon State University, Corvallis, OR 97331, USA. e-mail: mahrt@coas.oregonstate.edu
© Royal Meteorological Society, 2005.

variability while Essery *et al.* (2004) allow subgrid variability in terms of the tile approach where the snow cover varies between the subgrid tiles.

Nakai *et al.* (1999) treated partial snow cover by relating a water availability factor to the snow-cover fraction of the canopy. In this study, we apply this approach to the entire canopy–ground system through simple one-source representations used in most regional and large-scale models. These representations are based on the bulk aerodynamic method, the Penman method or the Penman–Monteith method. These formulations are physically incomplete but are commonly used in models that cannot accommodate more complex schemes nor obtain the spatial variation of the vegetation parameters required for more complex schemes. Such formulations have not been directly evaluated in terms of eddy-correlation measurements of the moisture flux over partial snow cover. We do not endorse these simpler formulations nor suggest replacement with more complex models, but rather evaluate them because they are often used in regional and large-scale models and are almost always used in operational models.

2. DATA

(*a*) *Instrumentation and initial processing*

To study sublimation from a non-melting snow surface and evaporation of snow melt, eddy-correlation data were collected above a surface sparsely covered by brush, a matted grass-covered surface and a snow-covered dry lake bed in the North Park Basin of Colorado, USA (Mahrt and Vickers 2005), during the FLuxes Over Snow Surfaces (FLOSSII) field programme as part of the Cold Land Processes Experiment. This study analyzes data collected by the Atmospheric Technology Division of the National Center for Atmospheric Research from 20 November 2002 to 2 April 2003. A 34 m tower was deployed at the grass site. Mean temperature and relative humidity were measured at eight vertical levels using ventilated T/RH sensors (Vaisala 50Y) with an aspiration system built by the Atmospheric Technology Division. Fast-response data for eddy-correlation fluxes were collected at 1, 2, 5, 10, 15, 20 and 30 m with Campbell CSAT3 sonic anemometers with axes aligned toward the west. Campbell KH20 Krypton hygrometers were installed at 2, 10, 20 and 30 m for computation of water vapour fluxes. Unless otherwise noted, this study analyzes eddy-correlation data from the 2 m level. The four components of the radiation budget were measured using up- and down-looking pyranometers for short wave (Kipp and Zonen) and up- and down-looking pyrgeometers for long wave (Epply). The downward-pointing pyrgeometer was used to estimate surface temperature. Eddy-correlation measurements at 2 m and radiation measurements were also taken over the brush, about 1.5 km north-north-east of the main tower and the dry lake site, about 1 km north-west of the grass site. The average height of the brush is about 0.5 m with a vegetation fractional coverage of 0.2 and total leaf area index of near unity.

The values of the soil heat flux in the primarily frozen ground were generally small (less than 5 W m^{-2}), except for sunny snow-free conditions in March when this term appears to be much larger. However, because of substantial missing data, the measurements of soil heat flux and water content could not be used for the statistical analyses of this study.

A modified version of the quality-control procedures in Vickers and Mahrt (1997) was applied. Many of the records removed by quality control are associated with snowfall or ice/frost on the instruments. For evaluation of models of the daytime moisture flux in this study, we include only hours from 1000 to 1500 local time.

We use only wind directions between 135° and 292°, to eliminate flow through the tower and eliminate the impact of heterogeneity of the surface north-north-west of the tower. This restriction, along with the requirement that all the data simultaneously pass the quality-control procedures at all three sites for each retained hour, reduces the dataset to 275 hours. The quality-control procedure eliminated about 25% of the data. For the regression analysis and model evaluation in the next section, we additionally removed cases of small net radiation (<10 W m^{-2}) and very small magnitude of the moisture flux ($<2 \times 10^{-3}$ g Kg^{-1} m s^{-1}), in order to eliminate cases with substantial relative errors in these two quantities, leaving 212 cases. Some evaluations of the models will be carried out separately for below-freezing and above-freezing conditions based on whether the three-station average of the 2 m hourly-averaged air temperatures was less than -1 °C or greater than 1 °C.

(*b*) *Snow fractional coverage*

The fractional snow cover is estimated from both the albedo based on the radiation sensors at the three sites and digital images from a camera at the top of the tower at the grass site aimed to the south, the primary wind direction. The images are characterized by varying brightness and quality. As a result, automated methods using a fixed brightness threshold for determining the existence of snow at each pixel, or applying a varying threshold based on a bimodal distribution of brightness, were not reliable. Therefore, the threshold for each image had to be selected based on inspection to best match snow and bare areas and exclude poor-quality segments of the image or other obstacles in the image. The snow fractional coverage is determined by the number of bright pixels exceeding the threshold, divided by total number of pixels. The field of view of the clipped images was limited to the grass south of the tower. Determination of the snow-cover fraction is contaminated by the changing view angle with distance from the tower. In addition, the field of view of the camera will be different from the footprints of the eddy-correlation measurements, which depend on height, wind speed and direction and stability.

The albedo is an incomplete indicator of the snow cover because it decreases with snow age even without a change of snow fractional coverage. In addition, the radiometer has a small surface footprint compared to that of the eddy-correlation measurements. In spite of these difficulties, the image-based snow-cover fraction and the albedo are highly correlated. Overall, the image-based snow-cover fraction and albedo explain about the same amount of variance of the water availability factors at all three sites, although the details depend on the method of estimating the potential evaporation as well as the site.

The image-based snow cover at the grass site seems to perform as well at the dry lake and brush sites as the site-specific albedos. Although the snow covers are usually significantly different at the three sites, they are well correlated. The details of the relationships of the water availability factors to the albedo and the image-based snow-cover fraction, as indicated by scatter diagrams, are somewhat different, partly due to the more bimodal distribution of the albedo compared to the image-based snow-cover fraction. With melting and sublimation, the albedo decreases due to both decreasing snow fractional coverage and decreasing albedo of the snow due to increasing snow age (increasing crystal size and particles on the snow surface). For cases when the image-based snow cover remained near 100% for multi-day periods, the albedo decreased at an average rate of 0.05 day^{-1}. As a result of the influence of snow age on albedo, there are fewer intermediate values of albedo compared with the image-based snow-cover fraction.

In subsequent analyses, we will use only the image-based fractional snow cover from the grass site to represent the regional snow-cover fraction, with the recognition that this snow-cover fraction is not absolute for the dry lake and brush sites and may cause biases in the estimate of the water availability factors. We will generally use image-based snow fractional coverage greater than 0.75 as an indicator of large snow-cover fraction for the region containing all three tower sites.

(*c*) *Surface flux estimates*

This study uses the height and stability-dependent averaging time formulated in Vickers and Mahrt (2003) to compute the perturbations. The fluxes are then averaged over one-hour periods to reduce random sampling errors. Since estimated tilt rotation angles of the sonic anemometers were small and the mean vertical motion shows reasonable vertical coherence, tilt corrections were not applied. To compute the sensible heat flux, the virtual heat flux from the sonic anemometer is corrected for moisture flux, although such a correction is small for the present data.

The Krypton Hygrometer data were adjusted with the Webb–Pearman–Leuning 'correction' (Webb *et al.* 1980) and also corrected for oxygen absorption. Time-lag corrections due to separation of the hygrometer and sonic anemometer were applied by maximizing the correlation coefficient for each individual record, subject to the maximum allowed lag of 0.5 s. Corrections for flux loss due to pathlength averaging and separation of the sonic anemometer from the Krypton Hygrometer are of uncertain reliability and are not applied here. The pathlength is 10 cm for the sonic anemometers and 2.4 cm for the krypton hygrometer while the separation distance between the centre of the two pathlengths is 27 cm. Extrapolation of cospectra to smaller scales indicates that the flux loss at 2 m due to pathlength averaging is generally unimportant for the daytime periods studied here.

Mahrt and Vickers (2003) found that the surface layer in the strongly stratified nocturnal boundary layer over a grass-covered surface could be less than 10 m, in which case the flux magnitude at the measurement height may be less than the surface flux. Based on vertical extrapolation of fluxes downward to the surface, such underestimation appears to be unimportant for most of the daytime conditions examined here, even though many of the cases are stably stratified.

3. Spatial variation of the moisture flux

The three eddy-correlation sites in FLOSSII allow examination of the moisture flux over grass-covered surfaces, sparse brush and bare ground (the dry lake bed). Averaged over the snow season, the moisture flux is about 20% greater over the brush than over the dry lake site and 11% greater than over the grass site, presumably due to greater average snow cover at the brush site associated with collection of blowing snow by the bushes. Blowing snow is collected in the form of drifts downwind from individual bushes and downwind from patches of bushes.

Moreover, the greater roughness and buoyancy generation of mixing at the brush site leads to greater mixing of moisture away from the surface than at other sites. The heat flux at the brush site is substantially greater than that for the dry lake and grass sites due to absorption of solar radiation by the partially or completely snow-free brush canopy (Fig. 1). The relatively low-albedo bushes efficiently capture solar radiation with low sun-elevation angle despite the small vegetation fraction of 0.2. Between-site differences of the moisture flux vary substantially from day to day. With strong winds

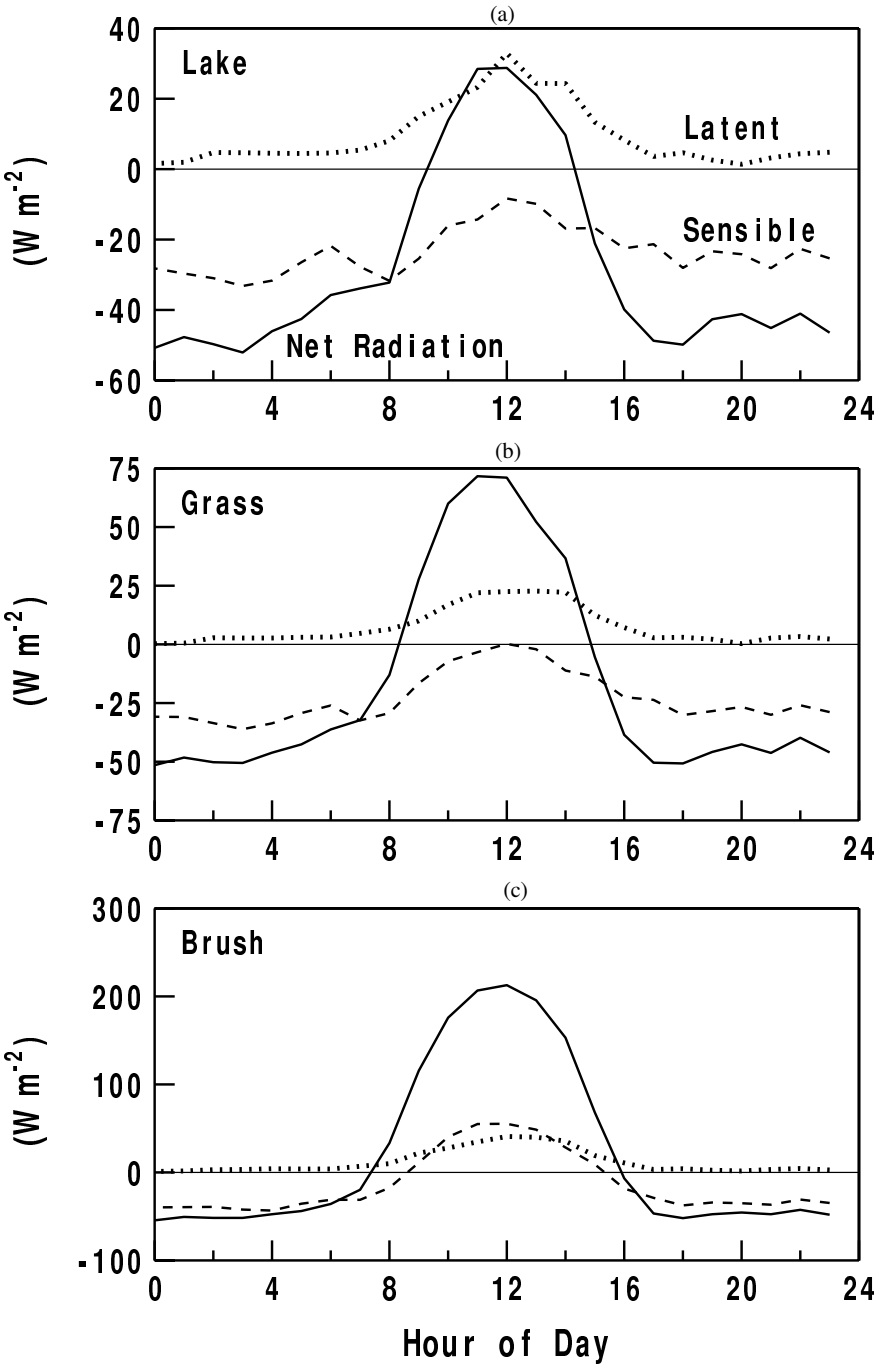

Figure 1. Diurnal variation of the net radiation, latent heat flux and sensible heat flux composited over the 20 snow-covered days with midday below-freezing conditions at the (a) dry lake, (b) grass and (c) brush sites. (Note changes in vertical scale.)

and complete snow cover, the sublimation is often greatest at the dry lake site where the surface is more exposed and saltation of snow is more likely.

The relative contributions of the downward sensible heat flux and net radiation to the heat available for sublimation and snow melt vary substantially between sites in the literature, ranging from dominance by net radiation to a few cases dominated by downward heat flux (see Table IV in Obleitner 2000), and at a given site vary with synoptic situation (Oerlemanns *et al.* 1999). Cline (1997) refers to snow-pack heat budgets for daytime melting conditions for sheltered sites with weak winds where the downward heat flux is more likely to be small compared to the net radiation. At high-latitude snow-covered sites, the averaged net radiation is small positive or negative and the sublimation/evaporation is driven primarily by downward heat flux (e.g. Bintanja 2000). King *et al.* (1996) find that for winter high-latitude conditions, the latent heat flux due to sublimation is small compared to downward sensible heat transfer towards the surface and net radiative cooling.

To examine the relative roles of radiation and downward heat flux for the present sites, we consider the surface energy budget in the form

$$\rho L_s \overline{w'q'} = R_{net} - G - M - \rho c_p \overline{w'\theta'}, \tag{1}$$

where perturbation quantities representing fluxes of moisture and sensible heat were derived as described in section 2(c), R_{net} is the net radiation, L_s is the sum of latent heat of fusion and vaporization (latent heat of sublimation), G is the heat flux into the snow–ground system, ρ is the mean air density, c_p is the specific heat capacity of the air and M is the heat used to melt snow for the part of the liquid water that percolates into the snow–ground system rather than evaporating. Such melted snow is not included in the latent heat flux term, as measured by the eddy-correlation system. M also includes energy released by refreezing of water at the surface, in which case M is negative. With more complete representation of the surface energy balance containing information on fractional coverage of melt water (Boone and Etchevers 2001), the evaporation of melt water can be explicitly predicted.

The above form of the surface energy balance (Eq. (1)) is valid for a very thin layer with negligible mass and thermal inertia as opposed to the heat budget for a layer of snow. This assumption becomes problematic with penetration of solar radiation into the snow surface and associated melting of sub-surface snow (Liston *et al.* 1999). Here, the sum of the melting term and the heat flux into the snow–ground system has been estimated as a residual of the surface energy budget, with the realization that such an estimate includes the errors in the net radiation and sensible and latent heat fluxes and includes the failure to close the surface energy budget due to different footprints of the measurements.

The diurnal variation of the surface energy budget at the dry lake site, with snow-cover fraction greater than 0.75, is separately composited for below-freezing and above-freezing conditions based on the 2 m hourly-averaged air temperatures. For snow-covered conditions, sufficient data to reduce the standard error well below the amplitude of the diurnal variation are available only for the below-freezing case (Fig. 1(a)). Here, the standard error is defined as the between-day standard deviation for a given hour divided by the square root of the number of days. This calculation of the standard error, here and elsewhere in this study, does not satisfy the strict definition of the standard error for an ensemble of data from the same statistical population. The composite for below-freezing conditions indicates that, for the 5-hour midday period when the net radiation is positive, the net radiation averages about 20 W m^{-2} while the downward sensible heat flux averages about 13 W m^{-2}. For the other 19 hours of the day, the

sublimation/evaporation is driven entirely by downward sensible heat flux, although the magnitude of the latent heat flux is substantially less than that for the midday period. For the midday period with below-freezing conditions, the residual of the surface energy budget is about 9 W m^{-2} energy surplus—about 1/3 of the net radiation. This surplus is thought to be only partly consumed by heat flux into the snow, G. Snow melt also occurs on some sunny below-freezing days, so that M may not be zero for below-freezing conditions.

For the other sites (Fig. 1), the contribution of downward sensible heat flux is less than that at the dry lake site. In fact at the brush site, the averaged sensible heat flux is significantly upward for the midday period due to heating of protruding vegetation. At the grass site for snow-covered conditions, the midday sensible heat flux averages near zero and is often weak downwards due to stable stratification associated with advection of heat from the upwind patches of brush (Mahrt and Vickers 2005).

4. Formulating the surface moisture flux

(*a*) *Bulk formula*

The bulk aerodynamic formulation and the stability-dependent Penman/ Penman–Monteith methods are both evaluated as estimates of the potential moisture flux. The Priestley–Taylor formulation was also examined but did not perform well, due partly to the importance of wind speed, and is not included in this study.

Applying Monin–Obukhov similarity theory to compute the transfer coefficient for moisture requires the aerodynamic surface moisture roughness length, theoretically defined in terms of extrapolation down to the roughness length using similarity theory for the non-dimensional moisture gradient (e.g. Sun *et al.* 1999). Aerodynamic surface moisture and temperature are normally not available from observations and never available in models.

As a consequence, the aerodynamic temperature is replaced with the surface radiation temperature. Such replacement redefines the transfer coefficients for heat and corresponding roughness length. The new transfer coefficients may be erratic and unpredictable, particularly over vegetation where the surface radiation temperature includes both sunlit and shady surfaces (see numerous references cited in Mahrt and Vickers 2004).

With use of the surface radiation temperature, the bulk aerodynamic formulations for heat and moisture become

$$\overline{w'\theta'} = C_h \overline{u}\{\theta_{\rm sfc} - \theta(z)\}, \tag{2}$$

$$\overline{w'q'} = C_q \overline{u}\{q_{\rm sat}(T_{\rm sfc}) - q(z)\}, \tag{3}$$

where the moisture flux formulation is now a prediction of the potential evaporation/transpiration (unlimited water availability), $T_{\rm sfc}$ is the surface radiation temperature, $\theta_{\rm sfc}$ is the corresponding surface potential temperature, q is the specific humidity and $\overline{u}$ the mean wind speed. C_h and C_q are the transfer coefficients for heat and moisture, respectively.

The prediction of the actual moisture flux is reduced from the potential value either by reducing the surface specific humidity (α approach)

$$\overline{w'q'} = C_q \overline{u}\{\alpha q_{\rm sat}(T_{\rm sfc}) - q(z)\}, \tag{4}$$

or by reducing the overall moisture flux by a single parameter, β, such that

$$\overline{w'q'} = \beta C_q \overline{u}\{q_{\rm sat}(T_{\rm sfc}) - q(z)\}, \tag{5}$$

where α and β will both be referred to as moisture availability factors. The α approach is physically more direct in that it attempts to correct for replacement of the aerodynamic surface specific humidity. However, it is vulnerable to errors particularly when the value of $\alpha q_{\rm sat}(T_{\rm sfc})$ is close to the value of $q(z)$, in which case the magnitude and even the sign of the predicted moisture flux is sensitive to the exact value of α. Consequently, the β approach may be more robust (Nappo 1975).

From Monin–Obukhov similarity theory, the transfer coefficients are estimated as:

$$C_h = \left[\frac{k}{\ln\{(z-d)/z_{0m}\} - \psi_m}\right]\left[\frac{k}{\ln\{(z-d)/z_{0T}\} - \psi_h}\right], \tag{6}$$

$$C_q = \left[\frac{k}{\ln\{(z-d)/z_{0m}\} - \psi_m}\right]\left[\frac{k}{\ln\{(z-d)/z_{0q}\} - \psi_q}\right], \tag{7}$$

where k is the von Kármán constant and z_{0m}, z_{0T} and z_{0q} are the roughness lengths for momentum, heat and moisture, respectively. The stability functions ψ_m, ψ_h and ψ_q are specified from Paulson (1970) for the unstable case and from Dyer (1974) for the stable case to be functions of z/L where L is the Obukhov length. The stability function for moisture is normally equated to that for heat. Although the displacement height, d, could be significant for drifting snow (Andreas 1995), its value could not be adequately estimated here. The displacement height is set to zero for the dry lake and grass sites and is crudely estimated to be 0.17 m for the 20–50 cm bushes at the brush site. A value of approximately half of the average brush height was used instead of the usual value of 2/3 because of the sparseness of the brush.

(*b*) *Roughness lengths*

Andreas *et al.* (2005) formulate the roughness length for snow by bridging the smooth-flow regime and strong-wind blowing-snow regime with an intermediate regime, where the aerodynamic roughness length depends on the micro-topography of the snow surface (Andreas 1995; Andreas and Claffey 1995; Bintanja and Reijmer 2001). The size of the present dataset for completely snow-covered conditions is probably too small to evaluate a three-term model of the roughness length.

The roughness lengths were estimated from the bulk formula using the observed fluxes and specified stability functions (section 4(a)). On average, the aerodynamic roughness length for momentum at the dry lake site for snow-covered conditions (Fig. 2) reaches a minimum for mean winds of about 4.5 m s^{-1}, with a sharp increase for low wind speeds. The increase of the aerodynamic roughness length for stronger wind speeds is relatively small, especially for above-freezing conditions. Generally the snow cover is sufficiently thin that drifting or large-amplitude undulations of the snow surface cannot develop without exposing bare ground, in which case the data are excluded from Fig. 2. The increase of the roughness length with decreasing wind speed for weak-wind conditions could be due to smooth-flow effects, although Mahrt *et al.* (1996) found such an increase for weak winds over water to be sensitive to the method of flux calculation.

For the grass site, the roughness length for momentum decreases substantially with increasing snow cover, but is nearly independent of snow cover at the brush site, where the snow depth was almost always shallow compared to the brush height. The roughness length at the dry lake site also varies little with snow cover since the bare surface, as well as the snow surface, both have small roughness length.

Since only snow-cover conditions are included in the roughness-length calculation, the water availability parameter is assumed to be unity, allowing estimation of the roughness length for moisture. Andreas *et al.* (2005) found that the ratio of the

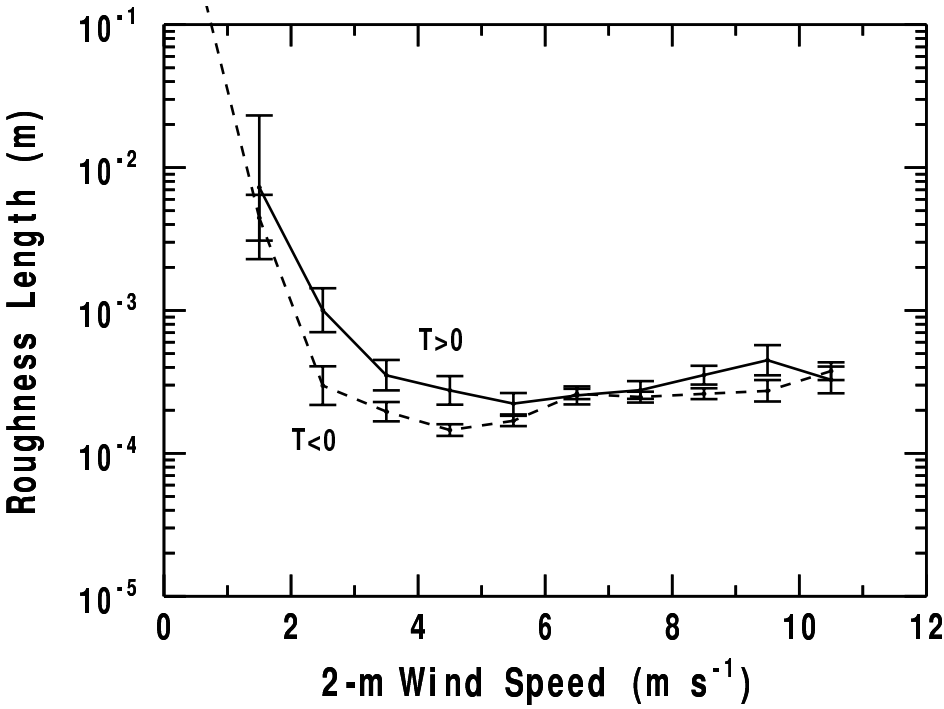

Figure 2. The dependence of the bin-averaged aerodynamic roughness length on wind speed for snow-covered conditions at the dry lake site for above-freezing (solid) and below-freezing (dashed) conditions. Bars denote +/− one standard error.

moisture roughness length to that for momentum over snow is greater than unity for small roughness Reynolds number and substantially less than unity for large roughness Reynolds number, although they note large scatter and additional uncertainty due to self-correlation. King and Anderson (1994) found that the moisture roughness length over the Antarctic ice shelf is greater than that for momentum and suggested that the influence of near-surface radiative flux divergence on the temperature profile influences the effective roughness lengths for temperature and moisture. For the present data, the roughness length for moisture for completely snow-covered conditions (water available factor assumed to be unity) is less than that for momentum, although a definite relationship between the two could not be established.

Since the water availability factor and the scalar roughness length cannot be simultaneously estimated from the data for partial snow cover and because the physical interpretation of the scalar roughness length is obscure for partial snow cover, we equate the roughness length for moisture to that for momentum for the analyses below. This eliminates the roughness length for moisture as a variable and avoids dependence of the water availability factor on the particular choice of the scalar roughness length.

(*c*) *Penman method*

Since use of the surface radiation temperature in the bulk formula often leads to erratic behaviour, Penman (1948) combined the bulk formula with the surface energy balance to eliminate surface temperature. Here, we employ the stability-dependent Penman approach to formulate the potential moisture flux from the snow surface and

any moisture flux from the soil:

$$E_{\mathrm{P}} = \frac{\Delta(R_{\mathrm{net}} - G - M) + \rho L_{\mathrm{s}} C_q \overline{u}\{q_{\mathrm{sat}}(T) - q\}}{\Delta + (C_h/C_q)}, \tag{8}$$

where

$$\Delta \equiv \frac{L_{\mathrm{s}}}{c_p}\frac{\mathrm{d}q_{\mathrm{sat}}}{\mathrm{d}T} \tag{9}$$

and where T is the air temperature and M and G are defined in Eq. (1). We will assume the stability-dependent transfer coefficients for heat and moisture are the same ($C_h = C_q$).

The actual evaporation is then estimated as

$$E = \rho L_{\mathrm{s}} \overline{w'q'} = \beta_{\mathrm{P}} E_{\mathrm{P}}, \tag{10}$$

where β_{P} is the water availability factor for the Penman relationship and is a function of the snow-cover fraction, vegetation state and soil moisture content.

(*d*) *Penman–Monteith relationship*

Monteith (1963) (see also Thom 1972, 1975 for a detailed derivation) later generalized the Penman formulation to include a resistance to represent the influence of stomatal control and soil moisture deficit. Since these models are often categorically used for all conditions, the influence of snow cover on the surface resistance should be examined. The stability-dependent Penman–Monteith relationship is written as

$$E_{\mathrm{PM}} = \rho L_{\mathrm{s}} \overline{w'q'} = \frac{\Delta(R_{\mathrm{net}} - G - M) + (\rho L_{\mathrm{s}}/r_{\mathrm{a}})\{q_{\mathrm{sat}}(T) - q\}}{\Delta + 1 + (r_{\mathrm{s}}/r_{\mathrm{a}})} \tag{11}$$

where r_{a} is the atmospheric resistance $1/(\overline{u}\, C_q)$, and r_{s} is the surface resistance, which here represents the influence of surface water availability. The vegetation was senescent for the duration of the field programme.

We have examined two versions of the stability-dependent Penman and Penman–Monteith methods. In the first version both the heat flux into the snow-ground system, G, and the melting term, M, are neglected. In the second version, the sum of G and M are estimated as the residual of the surface energy budget. In the first approach, the net available energy ($R_{\mathrm{net}} - G - M$) is overestimated, causing smaller values of the water availability factor for the Penman relationship and larger values of the surface resistance for the Penman–Monteith method. With the second approach, any underestimation of the latent and sensible heat fluxes would lead to overestimation of ($G + M$) and therefore underestimation of the net available energy. With suitably adjusted water availability factors and surface resistance, the two versions explain roughly the same amount of variance of the observed surface moisture flux. We proceed with the version of the potential evaporation based on inclusion of the heat flux into the ground and melting terms, by equating their sum to the residual of the surface energy balance, with the recognition that neither approach is ideal.

5. Water availability factors

(*a*) *Dependence on snow-cover fraction*

We now examine the behaviour of the water availability factors (α in Eq. (4), β in Eq. (5) and β_{P} in Eq. (10)), computed from the observed moisture flux and the potential

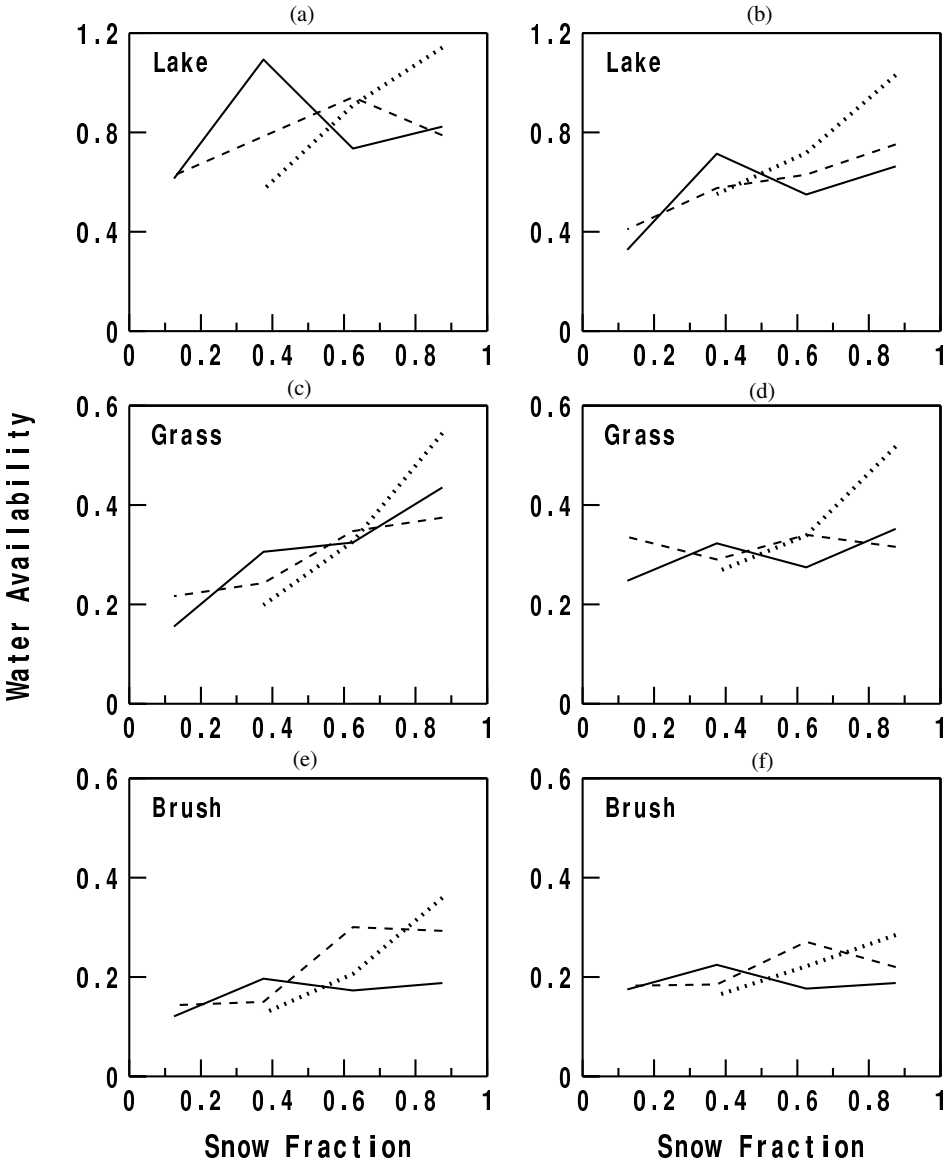

Figure 3. Dependence of the bin-averaged water availability factors on snow cover at the dry lake site for above-freezing (solid), below-freezing weak wind (<6 m s^{-1}, dashed) and below-freezing strong wind (>6 m s^{-1}, dotted), for (a) the β bulk formula and (b) the β_P Penman relationship. (c)–(d) and (e)–(f) are as (a)–(b), but for the grass and brush sites, respectively.

values computed from the bulk or Penman relationship for each hour. We also evaluate the resistance from the Penman–Monteith method (Eq. (11)).

Although the moisture flux itself decreases with increasing snow-cover fraction due to decreasing potential evaporation (reduced net radiation and decreased mixing), the water availability factors increase systematically with increasing snow-cover fraction at all three sites, at least for below-freezing conditions with significant wind (Fig. 3, Table 1). The relationship is strongest at the grass site where the soil is largely decoupled

TABLE 1. DEPENDENCE OF WATER AVAILABILITY PARAMETERS ON SNOW-FRACTIONAL COVERAGE, BASED ON LINEAR REGRESSION WITH NON-ZERO INTERCEPT FOR VANISHING SNOW COVER

	α from BA*			β from BA*			β_P from Penman			r_s (s m^{-1}) from P–M		
Site	Int.	Slope	R^2	Int.	Slope	R^2	Int.	Slope	R^2	Int.	Slope	R^2
Lake	0.78	0.24	0.29	0.57	0.42	0.25	0.74	0.25	0.16	39	−30	0.04
Grass	0.40	0.48	0.70	0.12	0.40	0.64	0.32	0.37	0.46	144	−100	0.27
Brush	0.45	0.32	0.43	0.10	0.19	0.35	0.22	0.13	0.16	132	−45	0.08

*Bulk aerodynamic.

from the atmosphere by the thick grass layer and remains frozen throughout most of the field programme. Therefore the soil probably does not contribute significantly to the moisture flux so that the water availability factor at the grass site becomes small when the snow cover vanishes. The closer relationship between the water availability and the snow-cover fraction at the grass site might also be influenced by the dominance of the snow-cover image by grass-covered areas.

The relationship of the water availability factors to snow-cover fraction is generally weaker for the dry lake and brush site where significant evaporation continues from the exposed wet soil after elimination of the snow cover. As a result, the zero-snow intercept in the regression relationship (Table 1) is larger at the dry lake site than at the grass site. The interpretation of the intercept for the brush site is more complex because of the influences of sunlit and shaded vegetation and sunlit and shaded soil.

The dependence of the water availability factors on snow-cover fraction is weak or undefinable for above-freezing conditions when the surface processes are more complex (Fig. 3). The water availability factors increase approximately linearly with snow-cover fraction for windy below-freezing conditions. The water availability factors were not sensitive to wind speed for above-freezing conditions.

Sublimation of blowing snow (e.g. Pomeroy and Essery 1999; Bintanja 2001; Liston and Sturm 2002, 2004) could not be isolated from the present moisture flux data. The enhancement of sublimation of suspended snow is thought to be due to increased surface area and greater ventilation around suspended particles compared to the ground snow surface, but self-controlled by increasing relative humidity due to the greater sublimation rate.

Much of the unexplained variance of the water availability factor is thought to be due to the influence of random flux errors on the hourly values of the estimated roughness length, inadequate measure of snow-cover fraction and the influence of blowing snow and special influences of melting, discussed below. The snow-cover fraction generally explains less of the variance of the moisture availability factor for the Penman and Penman–Monteith relationships than for the bulk formula. However, in terms of prediction of the moisture flux, the overall performance of the Penman and Penman–Monteith models is comparable to, or exceeds, that of the bulk formula (section 6).

(*b*) *Reduction of water availability*

The moisture flux above a snow-covered surface with no protruding vegetation is generally assumed to be close to the potential value. However, the water availability factors are generally substantially less than unity at the grass site, even with complete snow cover. We outline some possible explanations:

(i) The variable footprint of the 2 m eddy-correlation measurement may include some brush beginning about 100 m to the south of the grass tower site, not included in the footprint of the snow-cover measurement.
(ii) Sparse protruding grass blades at the grass site do not appreciably affect the snow-cover measurements but may partially shelter the snow, reducing the moisture flux below the potential value.
(iii) Equating the roughness length for moisture to that for momentum may overestimate the potential evaporation.
(iv) The moisture flux from older snow may be less than potential due to interference by particles on the snow surface.
(v) The observed moisture flux is underestimated due to flux loss associated with pathlength averaging (section 2) and instrument separation.
(vi) With melting conditions, a very thin stable boundary layer forms (Mahrt and Vickers 2005), such that the moisture flux at 2 m may be significantly less than that at the surface.
(vii) Based on evaluation of the Monin–Obukhov non-dimensional gradients for temperature and moisture, the transfer coefficient C_q appears to be less than that for heat.

Other unanticipated observational problems could also be important. The footprint of the eddy-correlation measurement cannot be estimated because the turbulence itself is heterogeneous, and the reliability of footprint theory is uncertain for stable conditions. Therefore explanation (i) cannot be evaluated, although we suspect it to be unimportant. The moisture roughness length could be tuned downwards to shift the water availability factor for snow-covered conditions towards unity. However, the scatter remains large and there appears to be no universal justification for such adjustments (section 4(b)) and explanation (iii) cannot be pursued. Based on section 2(c), explanation (vi) is probably not important. Flux loss due to pathlength averaging (explanation (v)) is also thought to be small (section 2(c)). Explanation (vii) is currently under investigation. The other explanations cannot be quantitatively estimated. The small water availability factors for large snow-cover fraction with melting were not anticipated since the Penman/Penman–Monteith relationships include the influence of inferred melting in the available energy and the melting constrains the surface temperature in the bulk aerodynamic formulation.

(*c*) *Vanishing snow cover*

With vanishing snow cover, the moisture flux remains significant at the dry lake site, presumably due to evaporation from the exposed wet soil. The evaporation from the soil at the grass site is expected to be small since the grass partially insulates the soil from the atmosphere. The water availability factor for the bulk formula at the grass site approaches asymptotically to about 0.1 with vanishing snow cover. The small remaining moisture flux could be due to some limited moisture flux from the soil, moisture stored in matted grass, extension of the footprint of the eddy-correlation measurement further upwind into the brush where drifted snow often remains and, finally, observational errors.

For vanishing snow cover, the potential evaporation for the bulk relationship increases sharply (Fig. 4), particularly at the grass and brush sites where the senescent vegetation heats up, corresponding to a rapid increase of the saturation specific humidity and potential moisture flux. The potential evaporation based on the Penman relationship also increases, partly due to increasing net radiation associated with decreasing albedo.

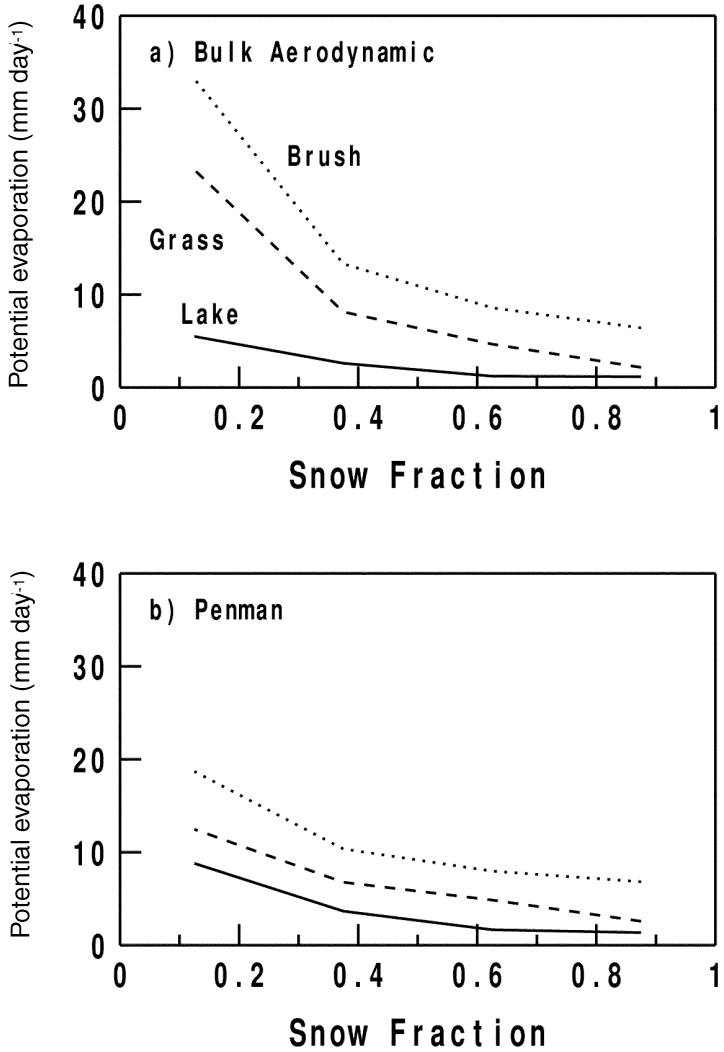

Figure 4. Dependence of the bin-averaged potential evaporation for the (a) bulk aerodynamic and (b) Penman methods for the three sites.

However, the potential evaporation for the Penman relationship increases less with decreasing snow cover than potential evaporation for the bulk formula. As a possible result, the water availability factor for the Penman relationship is greater and less variable than that for the bulk formula for snow-free conditions for the grass and brush sites (Fig. 3).

6. Evaluation of model performance

We now evaluate the skill of each method using the regression models for the water availability (Table 1). Model evaluations would be best carried out with independent data. In spite of the large available dataset, the wide variety of conditions, including variable snow cover, required use of the entire dataset for the formulation of the water availability factors as functions of snow-cover fraction.

TABLE 2. THE FRACTION OF VARIANCE (R^2) OF THE OBSERVED MOISTURE FLUX EXPLAINED BY LINEAR REGRESSION USING THE BULK AERODYNAMIC α AND β MODELS, THE PENMAN MODEL (β_P), AND THE PENMAN–MONTEITH MODEL (r_s)

Site	Bulk α	Bulk β	Penman β_P	P–M r_s
Lake	0.84 (1.04)	0.84 (0.74)	0.93 (0.43)	0.95 (0.37)
Grass	0.39 (2.91)	0.58 (0.98)	0.71 (0.76)	0.69 (0.78)
Brush	0.44 (5.89)	0.57 (1.20)	0.66 (0.83)	0.70 (0.77)
Lake	0.82 (1.56)	0.83 (1.27)	0.92 (0.54)	0.92 (0.46)
Grass	0.50 (6.68)	0.54 (3.21)	0.68 (1.32)	0.67 (0.93)
Brush	0.54 (9.71)	0.59 (2.78)	0.68 (1.04)	0.71 (0.84)

The parentheses enclose the r.m.s. error (mm day^{-1}).
The parametrizations of the water availabilities are based on linear regressions (Table 1) on the image-based snow-cover fraction from the grass site.
The lower half of the table results from the application of the averaged values of the water availabilities without dependence on snow-cover fraction.

The r.m.s. error (parentheses in Table 2) offers a more reliable evaluation of the models than the variance explained, since significant variance explained may still correspond to large bias. In terms of both r.m.s. error and variance explained, the bulk aerodynamic α model does not perform as well as the other models (Table 2). Small errors in the adjustment of the surface specific humidity (adjustment of α) can lead to large errors in the vertical difference of the specific humidity (Eq. (2)). As a result, the moisture flux predicted by the α approach varies much more than the observed moisture flux (Fig. 5). The α model often substantially overpredicts the moisture flux for cases of little or no snow cover and warm surface conditions (Fig. 6), corresponding to large saturation specific humidity. Correct prediction would require significantly smaller values of α for these specific cases. The α approach is particularly poor for the grass and brush sites where vegetation plays a role. We forgo attempts to design more complex formulations of α.

The bulk aerodynamic β model predicts more of the variance of the surface moisture flux with less r.m.s. error at the grass and brush sites than the α model (Table 2), but performs not as well as the stability-dependent Penman/Penman–Monteith formulations for all three sites. In addition, the β approach suffers substantially larger errors than the other approaches for cases when the saturation specific humidity at the surface temperature is close to the atmospheric specific humidity. That is, small errors in either one produce large errors in the vertical moisture difference. If the difference becomes approximately zero with significant moisture flux, the value of β becomes much greater than unity. These cases were eliminated by requirements on the minimum moisture flux and net radiation (section 2(a)). Their inclusion would have further degraded the performance of the β approach beyond that in Table 2.

The bulk aerodynamic β and α (Fig. 6) approaches seriously overpredict the moisture flux for cases of higher surface temperature due to rapid increase of the corresponding saturation specific humidity. These errors are even more serious when failing to include the dependence of α and β on snow cover, reflected in the statistics in the lower half of Table 2.

The Penman (Fig. 6) and Penman–Monteith methods do not suffer such overprediction, even when the dependence of β_P and r_s on snow cover are not included. This superior behaviour is due to elimination of the saturation specific humidity at the surface temperature. That is, in spite of the relatively weak dependence of the water availability factor on snow-cover fraction for the Penman and Penman–Monteith

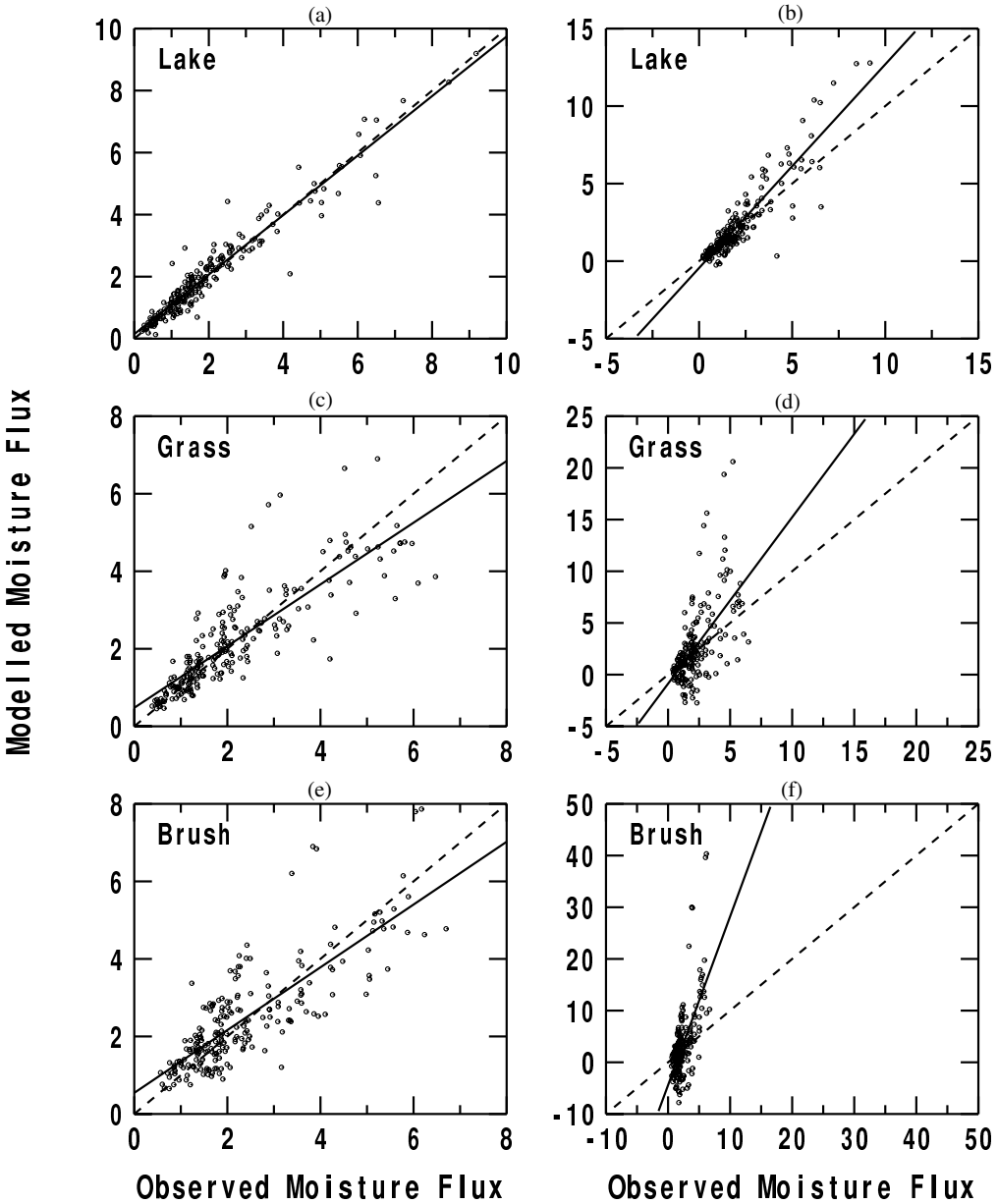

Figure 5. Modelled moisture flux (mm day^{-1}) for the dry lake site as a function of observed moisture flux with the linear regression (solid) and one-to-one (dashed) lines for (a) the Penman model and (b) the bulk aerodynamic α model. (c)–(d) and (e)–(f) are as (a)–(b), but for the grass and brush sites, respectively. (Note changes in scales.)

relationships (section 5), these relationships explain substantially more variance (substantially smaller r.m.s. error) of the moisture flux than the α and β approaches at the grass and brush sites. At these sites, $q_{\mathrm{sat}}(T_{\mathrm{sfc}})$ is physically complex due to contributions of the vegetation to the measured surface temperature and leads to unrealistically large variation of the predicted moisture flux using the α and β approaches.

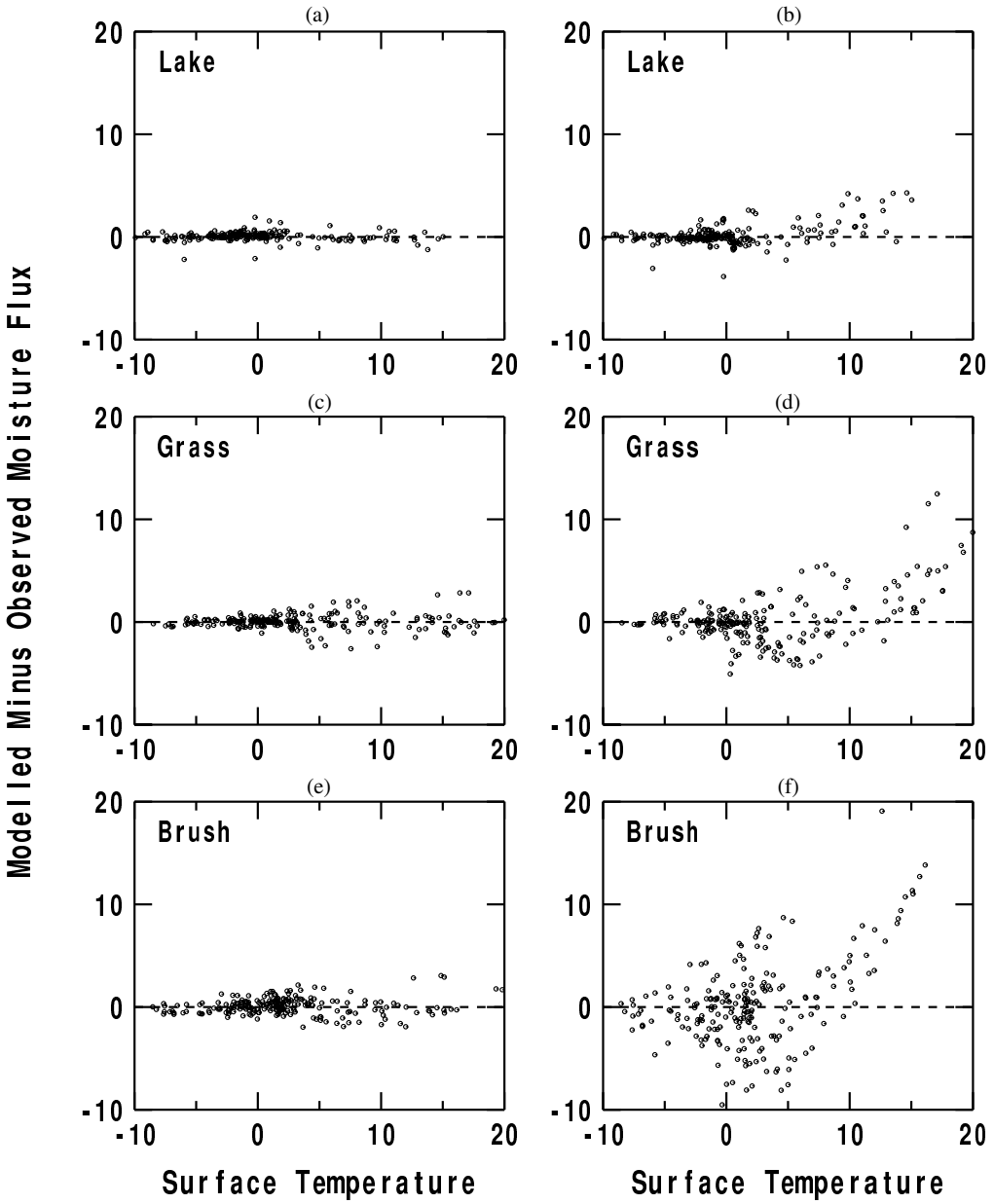

Figure 6. The error in the modelled moisture flux (mm day^{-1}) as a function of surface temperature (°C) at the dry lake site for (a) the Penman and (b) bulk aerodynamic α models. (c)–(d) and (e)–(f) are as (a)–(b), but for the grass and brush sites, respectively. In (f), four of the modelled flux values are large and off the scale.

7. CONCLUSIONS

The seasonal moisture flux is greatest above the brush site presumably because of the collection of blowing snow by the brush. The net radiation is also greater over the brush-covered surface due to absorption of solar radiation by the protruding vegetation and often produces significant midday upward sensible heat flux from the surface. The heat flux over the grass and dry lake sites for snow-covered conditions is generally

downward, even during the day, and therefore provides energy for sublimation/snow melt.

In this study, we have evaluated the simplest models of surface moisture flux which are commonly used in regional and large-scale models. The water availability factors for the bulk aerodynamic method and the Penman method and the surface resistance for the Penman–Monteith method all tend to increase with increasing snow fractional cover for all three sites. The water availability factors are larger and more closely related to fractional snow cover for below-freezing windy conditions, where the water availability factor increases approximately linearly with increasing snow cover.

The stability-dependent Penman and Penman–Monteith methods are better able to predict the moisture flux than the bulk aerodynamic method, particularly at the grass and brush sites. With higher surface temperatures and larger $q_{\mathrm{sat}}(T_{\mathrm{sfc}})$, the bulk aerodynamic α and β models seriously overpredict the moisture flux. While this overprediction is reduced by the inclusion of the dependence of α and β on water availability, the bulk formula is still inferior to the Penman and Penman–Monteith formulations even without inclusion of such dependencies in Penman/Penman–Monteith relationships.

Lee and Mahrt (2004) have evaluated a new two-source model using the present data. While the two-source approach includes more physics and partitions $q_{\mathrm{sat}}(T_{\mathrm{sfc}})$ into different contributions from the ground–snow–vegetation system, the different components cannot be directly evaluated from the data and their use requires information on the spatial distribution of vegetation parameters that sometimes must be inferred.

Acknowledgements

We gratefully acknowledge two anonymous reviewers, whose comments were more important than they probably anticipated. We also appreciate the extensive helpful comments of Ed Andreas, Glen Liston, Young-Hee Lee and Aaron Boone and the field assistance of the NCAR ATD staff. This material is based upon work supported by grant NAG5-11586 from the NASA Hydrology Program, grant DAAD19-0210224 from the Army Research Office and grant 0107617-ATM from the Physical Meteorology Program of the National Sciences Program.

References

Andreas, E. 1995 Air-ice drag coefficients in the Western Weddell Sea. II: A Model based on form drag and drifting snow. *J. Geophys. Res.*, **100,** 4821–4831

Andreas, E. 2002 Parameterizing scalar transfer over snow and ice: A Review. *J. Hydrol.*, **3,** 417–432

Andreas, E. and Claffey, K. 1995 Air-ice drag coefficients in the Western Weddell Sea. I: Values deduced from profile measurements. *J. Geophys. Res.*, **100,** 4833–4843

Andreas, E. L, Jordan, R. E. and Makshtas, A. 2005 Parameterizing turbulent exchange over sea ice: The Ice Station Weddell results. *Boundary-Layer Meteorol.*, **114,** 439–460

Bintanja, R. 2000 Surface heat budget of Antarctic snow and blue ice: Interpretation of spatial and temporal variability. *J. Geophys. Res.*, **105,** 24397–24407

2001 Modelling snowdrift sublimation and its effect on the moisture budget of the atmospheric boundary layer. *Tellus*, **53A,** 215–232

Bintanja, R. and Reijmer, C. 2001 A simple parameterization for snowdrift sublimation over Antarctic snow surfaces. *J. Geophys. Res.*, **106,** 31739–31748

Boone, A. and Etchevers, P. 2001 An intercomparison of three snow schemes of varying complexity coupled to the same land-surface and macroscale hydrologic models. Part I: Local-scale evaluation at an Alpine site. *J. Hydrol.*, **2,** 374–394

Cline, D. W. 1997 Snow Surface energy exchanges and snowmelt at a continental, midlatitude Alpine site. *Water Resources Res.*, **33,** 689–701

Davis, R. E., Hardy, J. P., Ni, W., Woodstock, C., McKenzie, J. C., Jordan R. and Li, X. 1997 Variation of snow cover ablation in the boreal forest: A sensitivity study on the effects of conifer canopy. *J. Geophys. Res.*, **102,** 29389–29395

Dyer, A. J. 1974 A review of flux-profile relationships. *Boundary-Layer Meteorol.*, **7,** 363–372

Essery, R., Pomeroy, J., Parvianen, J. and Storck, P. 2003 Sublimation of snow from coniferous forests in a climate model. *J. Climate*, **16,** 1855–1864

Essery, R., Best, M., Betts, R. and Cox, P. 2004 Explicit representation of subgrid heterogeneity in a GCM land surface scheme. *J. Hydrol.*, **4,** 530–543

Hedstrom, N. R. and Pomeroy, J. W. 1998 Measurements and modelling of snow interception in the boreal forest. *Hydrol. Processes*, **12,** 1611–1625

King, J. C. and Anderson, P. S. 1994 Heat and water vapor fluxes and scalar roughness lengths over an Antarctic ice shelf. *Boundary-Layer Meteorol.*, **69,** 101–121

King, J. C., Anderson, P. S., Smith, M. C. and Mobbs, S. D. 1996 The surface energy and mass balance at Halley, Antarctica, during winter. *J. Geophys. Res.*, **101,** 19119–19128

Lee, Y.-H. and Mahrt, L. 2004 An evaluation of snowmelt and sublimation over short vegetation in land surface modelling. *Hydrol. Processes*, **18,** 3543–3557

Link, T. E. and Marks, D. 1999 Point simulation of seasonal snow cover dynamics beneath boreal forest canopies. *J. Geophys. Res.*, **104,** 27841–27857

Liston, G. E. 1995 Local advection of momentum, heat and moisture during the melt of patchy snow covers. *J. Appl. Meteorol.*, **34,** 1705–1715

2004 Representing subgrid snow cover heterogeneities in regional and global models. *J. Climate*, **17,** 1381–1397

Liston, G. E. and Sturm, M. 1998 A snow-transport model for complex terrain. *J. Glaciol.*, **44,** 498–516

2002 Winter precipitation patterns in arctic Alaska determined from a blowing-snow model and snow-depth observations. *J. Hydrometeorol.*, **3,** 646–659

2004 The role of winter sublimation in the Arctic moisture budget. *Nordic Hydrol.*, **35,** 325–334

Liston, G. E., Winther, J.-G., Bruland, O., Elvehøy, H. and Sand, K. 1999 Below-surface ice melt on the coastal Antarctic ice sheet. *J. Glaciol.*, **45,** 273–285

Liston, G. E., McFadden, J. P., Sturm, M. and Pielke, R. A. 2002 Modelled changes in arctic tundra snow, energy and moisture fluxes due to increased shrubs. *Global Change Biol.*, **8,** 17–32

Mahrt, L. and Vickers, D. 2003 Formulation of turbulent fluxes in the stable boundary layer. *J. Atmos. Sci.*, **60,** 2538–2548

2004 Bulk formulations of the surface heat flux. *Boundary-Layer Meteorol.*, **110,** 357–379

2005 Boundary-layer adjustment over small-scale changes of surface heat flux. *Boundary-Layer Meteorol.*, in press

Mahrt, L., Vickers, D., Howell, J., Edson, J., Hare, J., Højstrup, J. and Wilczak, J. 1996 Sea surface drag coefficients in RASEX. *J. Geophys. Res.*, **101,** 14327–14335

Monteith, J. L. 1963 Pp. 95–112 in *Environmental Control of Plant Growth*, Ed. L. T. Evans, Academic Press, New York

Nakai, Y., Sakamoto, T., Terajima, T., Kitamura, K. and Shirai, T. 1999 The effect of canopy snow on the energy balance above a coniferous forest. *Hydrol. Processes*, **13,** 2371–2382

Nappo, C. J. 1975 Parameterization of surface moisture and evaporation rate in a planetary boundary layer model. *J. Appl. Meteorol.*, **14,** 289–296

Obleitner, F. 2000 The energy budget of snow and ice at Breidamerkurjökull, Vatnajökull, Iceland. *Boundary-Layer Meteorol.*, **97,** 385–410

Oerlemans, J., Bjørnsson, H., Kuhn, F., Obleitner, F., Palsson, F., Smeets, C. J. P. P., Vugts, H. F. and De Wolde, J. 1999 Glacio-meteorological investigations on Vatnajökull, Iceland, summer 1996: an overview. *Boundary-Layer Meteorol.*, **92,** 3–26

Paulson, C. A. 1970 The mathematical representation of wind speed and temperature profiles in the unstable atmospheric surface layer. *J. Appl. Meteorol.*, **9,** 857–861

Penman, H. L. 1948 Natural evaporation from open water, bare soil, and grass. *Proc. R. Soc. London*, **A193,** 120–145

Pomeroy, J. W. and Essery, R. H. L. 1999 Turbulent fluxes during blowing snow: field test of model sublimation predictions. *Hydrol. Processes*, **13,** 2963–2975

Pomeroy, J. W., Toth., B., Granger, R., Hedstrom, N. and Essery, R. 2003 Variation in surface energetics during snowmelt in a subarctic mountain catchment. *J. Hydrometeorol.*, **4,** 702–719

Sturm, M., McFadden, J. P., Liston, G. E., Chapin III, F. S., Racine, C. H. and Holmgren, J. 2001 Snow–shrub interactions in arctic tundra: A hypothesis with climatic implications. *J. Climate*, **14,** 336–344

Sun, J., Massman, W. and Grantz, D. 1999 Aerodynamic variables in the bulk formulation of turbulent fluxes. *Boundary-Layer Meteorol.*, **91,** 109–125

Thom, A. S. 1972 Momentum, mass and heat exchange of vegetation. *Q. J. R. Meteorol. Soc.*, **98,** 124–134

1975 Momentum, mass and heat exchange of plant communities. In *Vegetation and the Atmosphere, Vol. I*, Ed. J. L. Monteith. Academic Press, New York, USA

Vickers, D. and Mahrt, L. 1997 Quality control and flux sampling problems for tower and aircraft data. *J. Atmos. Oceanic Technol.*, **14,** 512–526

2003 The cospectral gap and turbulent flux calculations. *J. Atmos. Oceanic Technol.*, **20,** 660–672

Webb, E. K., Pearman, G. I. and Leuning, R. 1980 Correction of flux measurements for density effects due to heat and water vapour transfer. *Q. J. R. Meteorol. Soc.*, **106,** 85–100

Yang, Z.-L., Dickenson, R., Hahmann, A., Niu, G.-Y., Shaikh, M., Gao, X., Bales, R., Sorooshian, S. and Jin, J. 1999 Simulation of snow mass and extent in general circulation models. *Hydrol. Processes*, **13,** 2097–2113